科学通报 2025 年 第 70 卷 第 27 期: 4744 ~ 4751
石墨烯材料的制备与应用专题 论 文
《中国科学》杂志社 SCIENCE CHINA PRESS

高温重熔化学气相沉积制备球形蒙烯铜粉

武文鑫[1,2], 冯庆康[2], 武旭红[3], 赵一沣[4], 张思洁[4], 时志远[4*], 郭新立[1*], 于庆凯[2,4,5*]

1. 江苏省先进金属材料高技术研究重点实验室, 东南大学材料科学与工程学院, 南京 211189
2. 上海氢田新材料科技有限公司, 上海 200444
3. 陕西斯瑞新材料股份有限公司, 西安 710077
4. 集成电路材料全国重点实验室, 中国科学院上海微系统与信息技术研究所, 上海 200050
5. 中国科学院大学材料科学与光电技术学院, 北京 100049
* 联系人, E-mail: shizhy@mail.sim.ac.cn; guo.xinli@seu.edu.cn; qyu@mail.sim.ac.cn

2024-12-31 收稿, 2025-04-17 修回, 2025-04-20 接受, 2025-04-21 网络版发表
国家重点研发计划(2023YFB4005200)资助

摘要 球形铜粉在增材制造、柔性电子、电接触材料等领域的广泛应用要求其具有高球形度、高流动性和高抗氧化性. 典型球化工艺面临铜液滴粘连, 导致球形度不高、卫星粉、粉体粒径分布宽等问题. 此外, 先球化后包覆工艺路径复杂且制备周期长. 在粉体球化的同时引入功能包覆层不仅可以降低粉体粘连, 而且可以同步实现球形铜粉功能化. 石墨烯与铜的界面润湿性差, 其作为“蒙皮”可避免粉体粘连, 而且其高电子迁移率、抗水氧渗透特性可赋予其高电导、抗氧化等卓越性能. 本文提出高温重熔化学气相沉积技术, 铜粉和甲烷在高温立式炉中相向流动, 同步实现高球形度铜粉制取及铜表面高质量石墨烯薄膜包覆. 该方案耦合粉体球化(铜熔化并在表面张力作用下球化)过程和石墨烯生长(铜液滴表面甲烷裂解实现碳形核生长)过程. 最终, 在1400°C下获得球形度达0.89±0.11的高球形化铜粉体. 石墨烯(层数在10层以内)层间的有序排列结构表明其具有较高的结晶质量. 与裸铜粉相比, 蒙烯铜粉在经过NaOH腐蚀处理或空气氧化处理后, 展现出更好的抗氧化性能. 本文提出的高温重熔化学气相沉积技术可连续制备具有高球形度、高氧化温度的蒙烯铜粉, 有望成为规模化制备高性能球形铜粉的通用技术, 为其广泛应用提供材料基础.

关键词 化学气相沉积技术, 石墨烯, 球形铜粉, 抗氧化

球形铜粉因其高导电性、优良热性能和均匀粒径等优异特性, 在增材制造[1~3]、粉末冶金[4,5]、电子产品[6]和热喷涂[7]等领域备受关注. 通过气体/水雾化[8,9]、等离子体雾化/球化[10]等方法, 可以实现球形铜粉体制备, 但仍然面临产品粒度分布较宽、卫星球、空心球、细粉收得率低等挑战. 此外, 微纳铜粉面临的易氧化问题会显著降低其性能和表现. 在铜表面形成一层功能涂层, 如有机聚合物[11]或碳材料[12], 可以改善其抗氧化性. 石墨烯作为一种原子层薄二维材料, 具有优异的导电性、导热性、抗水氧渗透等特性[13,14], 以少层石墨烯为功能“蒙皮”可有效保持或增强铜基体性能[15~20]. 通过高能球磨法、纳米分散法等“自上而下”的复合方式将铜粉和石墨粉进行混合是一种普遍的复合手段[21~23], 然而实现稳定而均匀的分散并保证石墨烯结构完整仍存在较大挑战.

基于化学气相沉积(chemical vapor deposition, CVD)方法, 利用固体碳源包覆或粉末隔离等策略防止铜粉烧结, 以“自下而上”的复合方式可以实现高质量石墨烯制备及有效复合[24~29]. 对于固态碳源法, 通常将固体碳源溶于溶剂并涂覆在铜粉表面, 之后将铜粉

引用格式: 武文鑫, 冯庆康, 武旭红, 等. 高温重熔化学气相沉积制备球形蒙烯铜粉. 科学通报, 2025, 70: 4744–4751
Wu W, Feng Q, Wu X, et al. Synthesis of spherical graphene-skinned copper powders by high-temperature remelting chemical vapor deposition (in Chinese). Chin Sci Bull, 2025, 70: 4744–4751, doi: 10.1360/TB-2024-1404

在高温下进行石墨烯生长, 但所得石墨烯质量较差, 含有较多无定型碳. 对于粉末隔离法, 通常采用氧化物颗粒隔离铜粉体, 之后在高温下进行石墨烯生长, 但后续异质粉末分离提高了工艺成本. 更重要的是, 典型的制备工艺都要求原料铜粉为高球形度铜粉体, 这显著增加了工艺成本. 流化床法可以耦合铜粉体球化和石墨烯包覆, 此前已有报道利用流化床法在1200°C下实现球形铜粉表面石墨烯生长[29]. 然而, 所得石墨烯铜粉表面存在较多的卫星球, 这可能与反应温度及粉体粒径分布相关.

本文基于微粒重熔原理[30]提出高温重熔CVD法. 利用外加温和的高温场, 使铜颗粒在分散下落过程中与气态碳源相互作用. 一方面, 通过热交换使颗粒熔化并在表面张力的作用下自发收缩为球形液滴; 另一方面, 铜液滴催化气态碳源裂解并在铜表面实现碳原子扩散和形核继而生长石墨烯. 通过调控生长温度, 一方面可以调控铜粉体球形度, 另一方面可以调控蒙烯铜粉体表面石墨烯形态及结晶性. 最终, 在1400°C生长温度下, 实现少层石墨烯覆盖的蒙烯铜粉体生长, 且显著提升铜粉体氧化温度. 该高温重熔CVD技术有望规模化制备蒙烯铜粉, 为其在增材制造等领域拓展应用空间.

1 实验方法

1.1 球形蒙烯铜粉制备方法

高温重熔CVD生长系统由三段加热立式炉为基础, 以2英寸刚玉管为气体上升和铜粉体下落通道. 上端为铜粉体输送系统, 下端为蒙烯铜粉体收集系统. 本文所用的典型反应温度设定为1400°C, 在升温阶段, 1000标准立方厘米(standard cubic centimeter per minute, sccm)氩气(argon, Ar)被通入到反应腔室,达到反应温度后, 补充通入14 sccm甲烷(methane, CH_4)和14 sccm氢气(hydrogen, H_2)以进行石墨烯生长. 铜粉(中诺新材, 纯度99.9%, 粒径为200目或325目)从上端落入反应区, 反应气氛自下端向上输送, 和铜粉形成气(反应气)-液(铜液滴)反应空间. 在下落过程中, 粉末在高温作用下迅速熔化和球化, 同时发生了CH_4的分解以及石墨烯的成核和生长. 随后, 蒙烯铜粉落入底部冷端, 由于铜粉表面蒙有石墨烯, 可以阻止铜粉体再次烧结. 最终, 在收集系统中得到流动性好的蒙烯铜粉体.

1.2 球形蒙烯铜粉表征方法

蒙烯铜粉表面形貌通过扫描电子显微镜(scanning electron microscope, SEM, JEOL JSM-7800F, 测量电压为15 kV)进行表征. 铜粉表面石墨烯结晶性通过拉曼谱仪(Raman spectroscopy, Raman, Thermo Fisher DXR, 532 nm, 室温测量)进行评估. 将蒙烯铜粉浸入0.5 mol/L $(NH_4)_2S_2O_8$水溶液3小时, 随后利用去离子水清洗3次, 用镍载网捞出以进行后续透射电子显微镜(transmission electron microscope, TEM, JEOL JEM-2100F, 测量电压为200 kV)表征其层数和层间堆垛次序. 原始/蒙烯铜粉体粒径通过激光粒度仪(Malvern Panalytical, Mastersizer 3000)进行测量. 原始/蒙烯铜粉的氧化性评估分别通过NaOH腐蚀和热重分析进行. 其中, 原始/蒙烯铜粉体分别在0.1 mol/L NaOH水溶液处理6和24小时, 随后利用去离子水清洗3次并进行抽滤以收集腐蚀后铜材料; 热重分析通过热重分析仪(thermogravimetry analysis, TG, Netzsch, STA449 F5)进行测量.

2 结果与讨论

2.1 不同生长温度下球形蒙烯铜粉体制备

基于高温重熔CVD技术(图1(a)), 在高温环境下构建气(CH_4)-液(铜液滴)反应空间, 实现蒙烯铜粉体快速生长. 铜粉体自上而下运动, 由固相转变为液相并在表面张力作用下迅速球化; CH_4自下而上通入, 高温及铜液滴催化促进CH_4裂解并释放碳原子, 随之在铜液滴表面形核生长形成石墨烯. 熔融铜表面提高了碳原子和氢原子的扩散及迁移速度, 确保碳原子供应, 液相表面还有利于石墨烯晶粒的旋转、排列和移动[24]. 此外, 反应气氛向上流动减缓铜粉下落速度, 延长气-液作用时间. 在这一过程中, 生长温度决定了铜粉体的固-液转变效率及球化速度, 决定了CH_4裂解和碳原子扩散、形核及生长速度, 是控制生长的关键因素.

图1(b)~(d)为不同处理温度下的铜粉体形貌SEM图像. 在1200°C下, 铜粉体更多呈现椭球形, 当处理温度升高至1400°C, 铜粉体基本为正球形. 为讨论粉体球形度, 基于ImageJ数据处理软件对SEM图像进行二值化处理[31], 进而提取不同处理温度下所得蒙烯铜粉体球形度数据(图1(e)). 可以看出, 随着处理温度升高, 铜粉体球形度由0.76±0.14逐渐提升至0.89±0.11. 在1400°C条件下处理不同初始粒径铜粉体, 可以实现粒径相对

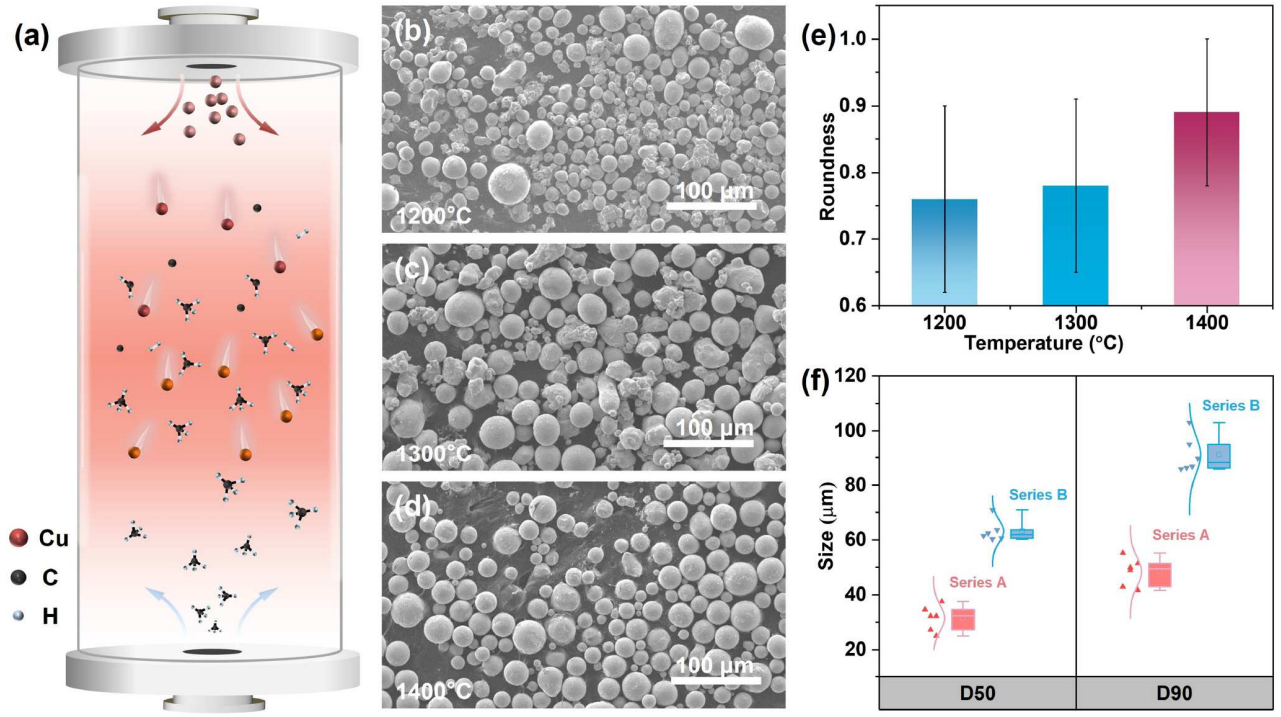

图 1 (网络版彩色)球形蒙烯铜粉制备方法及形态分析. (a) 高温重熔化学气相沉积技术示意图; (b)~(d) 在1200°C (b), 1300°C (c), 1400°C (d)处理温度下所得蒙烯铜粉体的SEM图像; (e) 不同处理温度下所得蒙烯铜粉体球形度结果; (f) 两类蒙烯铜粉体的粒径分布结果

Figure 1 (Color online) Synthesis of spherical graphene-skinned Cu powder and its morphology analysis. (a) Schematic of high-temperature remelting chemical vapor deposition; (b)–(d) SEM images of spherical graphene-skinned Cu powder synthesized at 1200°C (b), 1300°C (c), and 1400°C (d), respectively; (e) roundness of spherical graphene-skinned Cu powder synthesized at different temperatures; (f) particle size distribution of two types of spherical graphene-skinned Cu powder

可控的球形蒙烯铜粉. 为统一评价粉体粒径分布, 选取一个样品的累计粒度分布百分数达到50%时所对应的粒径(中值粒径, D50)作为评价参数. 面向增材制造或熔渗烧结工艺对铜粉体粒径尺寸需求, 选取两种不同粒径分布的铜原料(Series A和Series B), 经过高温生长后可获得中值粒径分布在25~40 μm (Series A)和60~80 μm (Series B)范围的两类蒙烯铜粉(图1(f)). 统计两类粉体累计粒度分布百分数达到90%时(D90)的粒径尺寸, 可以发现尺寸分布未有明显增加, 表明粉体粒径分布区间窄的特点. 这为蒙烯铜粉体应用奠定了良好的材料基础.

在实现铜粉体形态控制的基础上, 进一步讨论高温熔融过程中气-液界面石墨烯生长情况(图2). 选取不同生长温度下球形蒙烯铜粉, 对其表面石墨烯进行形态和结晶性分析. 图2(a)~(c)分别为不同生长温度下的蒙烯铜粉体的SEM图像, 与之对应的局部放大图像如图2(a_1)~(c_1)所示. 在1200°C下, 铜粉表面难以看到石墨烯薄膜形态, 多为裸露铜表面, 零星分布少许碳物质. 随着生长温度进一步升高, 在1300°C下可以看到不连续薄膜(图2(b_1)中深色区域); 当生长温度达1400°C时, 铜粉表面可以得到连续薄膜(图2(c_1)). Raman作为一种通用的石墨烯层数和结晶度的快速表征方法, 可以对单颗粒蒙烯铜粉体表面石墨烯进行结晶度评价[29]. 如图2(d)所示, 在不同生长温度下, 铜粉表面石墨烯Raman的2D峰强度均明显低于G峰, 所得石墨烯呈现多层特点. 随着生长温度增高, 2D峰强度显著提高, D峰和G峰的峰面积比例(I_D/I_G)逐渐降低, 表明铜粉表面石墨烯结晶性随反应温度升高而提升. 本文后续针对1400°C生长条件下所得蒙烯铜粉体, 对其表面石墨烯层数及粉体抗氧化性展开讨论.

2.2 球形蒙烯铜粉体结构及抗氧化性表征

对于高温重熔过程, 原料铜颗粒在下落过程中的碰撞及融合决定了所得蒙烯铜粉体形态. 如图3(a)为生长过程所采用的原料铜颗粒SEM图像, 可以看出其形态多为球形度较低的不规则多面体. 经历高温重熔及

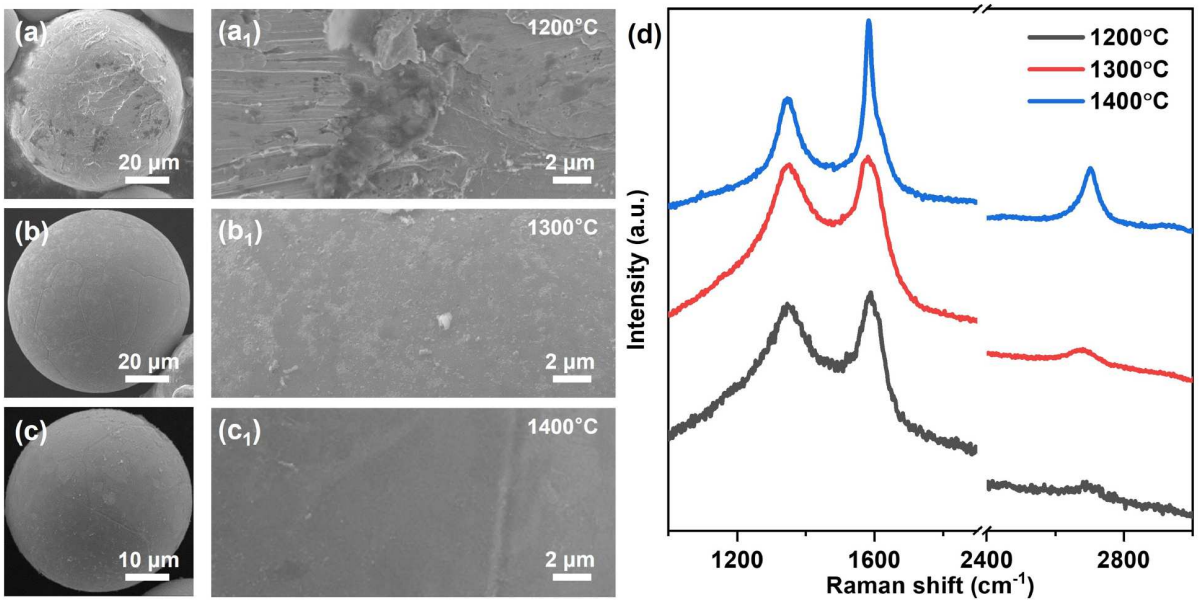

图 2 (网络版彩色)温度相关的球形蒙烯铜粉体及其表面石墨烯. (a)~(c) 在1200°C (a), 1300°C (b), 1400°C (c)处理温度下所得单个球形蒙烯铜粉颗粒的SEM图像; (a1)~(c1) 与图(a)~(c)对应的局部放大SEM图像; (d) 球形蒙烯铜粉体表面石墨烯的Raman测量结果

Figure 2 (Color online) Temperature-dependent spherical graphene-skinned Cu powder and the graphene on its surface. (a)–(c) SEM images of single spherical graphene-skinned Cu powder synthesized at 1200°C (a), 1300°C (b), and 1400°C (c), respectively; (a1)–(c1) zoomed-in SEM images corresponding to figures (a)–(c); (d) typical Raman spectra of temperature-dependent spherical graphene-skinned Cu powder

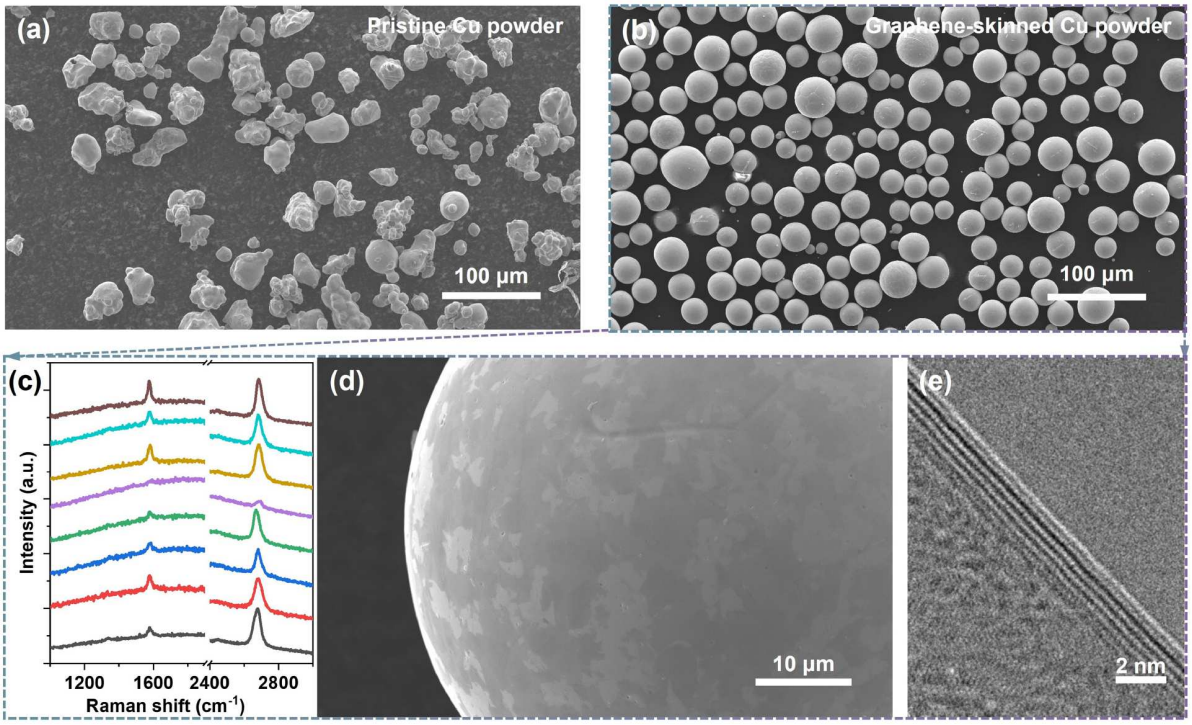

图 3 (网络版彩色)球形蒙烯铜粉典型结果. (a), (b) 裸铜粉体(a)、蒙烯铜粉体(b)的SEM图像; (c) 单颗粒蒙烯铜粉体表面不同位置Raman谱线; (d) 单颗粒蒙烯铜粉体局部放大的SEM图像; (e) 湿法转移所得石墨烯TEM图像

Figure 3 (Color online) Typical results of spherical graphene-skinned Cu powder. (a, b) SEM images of pristine Cu powder (a), and graphene-skinned Cu powder (b); (c) Raman spectra of single graphene-skinned Cu powder; (d) zoomed-in SEM image of single graphene-skinned Cu powder; (e) TEM image of graphene layers obtained from the wet-transfer process

碳材料生长后, 其转变为球形度高的蒙烯铜粉体(图3(b)). 激光粒度仪测量结果显示, 生长前后铜粉体的中值粒径(D50)分别为25.8和32.3 μm. 这表明, 在该工艺条件下, 铜粉体生长过程中的融合长大现象不显著. 进一步, 对球形蒙烯铜颗粒表面石墨烯覆盖度、形态及结构进行分析. 由于蒙烯铜颗粒的曲面特点及石墨烯厚度较低, 常规的元素面分布图测量具有较大误差. 在此, 随机选取蒙烯铜颗粒表面6~8个测量点进行石墨烯覆盖度判定. 图3(c)为蒙烯铜颗粒表面不同位置Raman谱线. 可以看出, 其不同位置均有较强的石墨烯Raman信号, 具有显著的2D峰, G峰强度高且锐利, D峰强度较低, 可以推测其表面覆盖了相对连续石墨烯薄膜且具有良好的结晶性. 通过SEM测量可以看出, 铜粉表面石墨烯存在衬度差异(图3(d)). 这一方面是由于曲面测量的误差, 另一方面也表明所得石墨烯厚度均匀性仍有待改善. 利用0.5 mol/L $(NH_4)_2S_2O_8$腐蚀处理去除铜基体以分离表面石墨烯. 如图3(e)所示, TEM测量结果显示所得石墨烯片层厚度为6层, 每层中的碳原子可清晰分辨, 层与层之间具有良好的排列结构, 这也说明了石墨烯具有良好的结晶性.

具有抗氧化环境腐蚀性能和高氧化温度的蒙烯铜粉体是面向铜腐蚀防护或铜浆料空气固化等实际应用的关键要素. 针对蒙烯铜粉体抗氧化性评价, 本工作通过NaOH腐蚀[32]和热重分析[33,34]两方面进行讨论. 将裸铜粉体浸入0.1 mol/L NaOH水溶液6小时, 腐蚀处理后其表面满覆盖针状铜氧化物(CuO及Cu_2O)(图4(a), (b)), 表明裸铜粉体表面发生严重氧化[32]. 将蒙烯铜粉体在0.1 mol/L NaOH水溶液中处理24小时, 与裸粉体相比, 蒙烯铜粉体表面针状铜氧化物密度显著降低(图4(c), (d)), 推测包覆的少层石墨烯改善了铜粉体抗氧化环境腐蚀能力. 分析处理前后Rama结果(图4(e)), 经过长时间NaOH腐蚀处理后, 石墨烯的D峰强度未明显增强, G峰和2D峰形态未发生明显变化, 这表明石墨烯具有良好的结构稳定性. 铜粉在空气中加热时的质量和焓的变化可有效反映其氧化特性. 通过热重分析, 选取重量增加1.0%所对应的温度作为铜粉的特征氧化温度[33]. 如图4(f)所示, 裸铜粉体和蒙烯铜粉体的特征氧化温度分别为366和455°C, 表明球形蒙烯铜粉在空气中的氧化温度高于裸铜粉体, 这可能来源于石墨烯包覆阻隔了氧气渗透至铜表面, 也可能是由于石墨烯

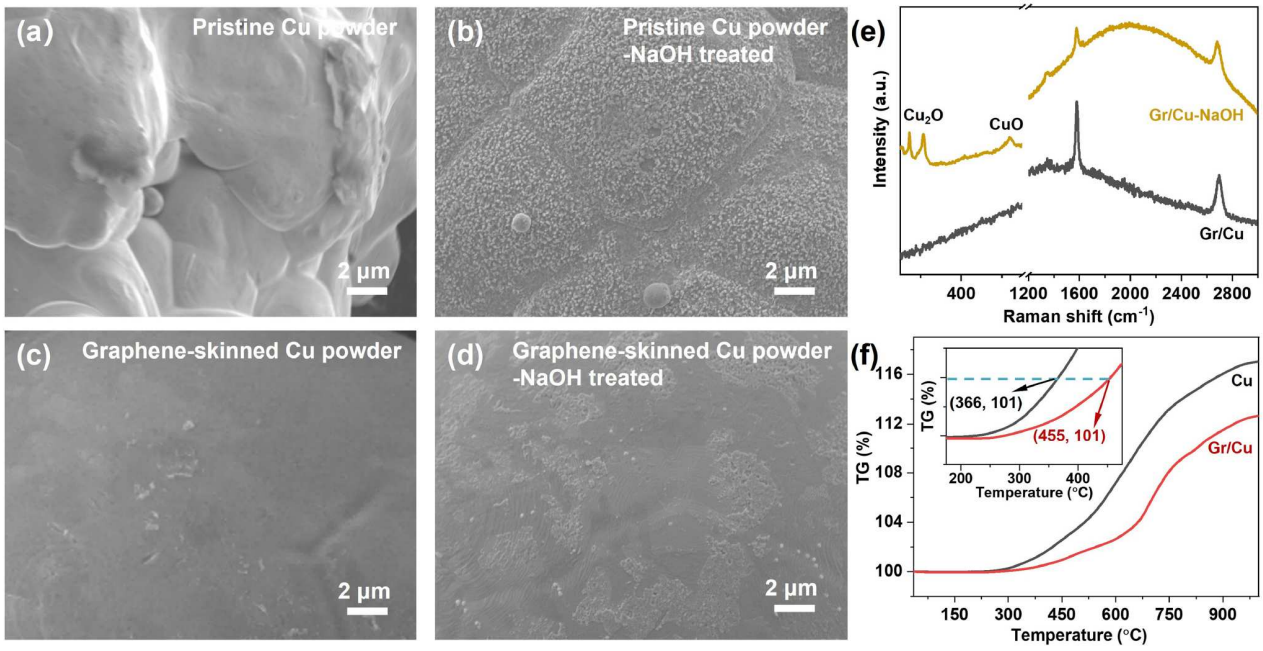

图 4 (网络版彩色)球形蒙烯铜粉抗氧化性能. (a), (b) NaOH腐蚀处理前(a)和处理后(b)裸铜粉体SEM图像; (c), (d) NaOH腐蚀处理前(c)和处理后(d)蒙烯铜粉体SEM图像; (e) NaOH腐蚀处理前后蒙烯铜粉体表面Raman谱线; (f) 裸铜粉体和蒙烯铜粉体热重分析曲线, 插图为局部放大

Figure 4 (Color online) Antioxidation behavior of spherical graphene-skinned Cu powder. (a), (b) SEM images of pristine Cu powder before (a) and after (b) NaOH corrosion treatment; (c), (d) SEM images of pristine graphene-skinned Cu powder before (c) and after (d) NaOH corrosion treatment; (e) Raman spectra of graphene-skinned Cu powder before and after NaOH corrossion treatment; (f) TG curves of pristine and graphene-skinned Cu powders, and the inset shows the partial enlargement curves

自身抗氧化性能较强，改善了蒙烯铜粉体的特征氧化温度[34].

3 结论

本文提出高温重熔CVD方法，在外加高温场环境下，通过构建气(CH_4)-液(铜液滴)反应空间，一方面加热铜颗粒使其熔化并球化，另一方面利用铜液滴催化CH_4裂解并在液态表面快速扩散形核以实现石墨烯生长. 在1400°C生长温度下，所得蒙烯铜粉呈正球形，球形度高达0.89±0.11. 蒙烯铜粉表面石墨烯层数在10层以下且具有良好的层间排列结构. 基于NaOH腐蚀处理及热重分析，蒙烯粉体呈现更高的抗氧化腐蚀能力和更高的氧化温度，其特征氧化温度(重量增加1.0%所对应的温度)较原始铜粉体提高了近90°C. 综上，本文所得蒙烯铜粉体拓展了其在增材制造、电子浆料和电接触材料等领域的应用前景.

参考文献

1 Godina R, Ribeiro I, Matos F, et al. Impact assessment of additive manufacturing on sustainable business models in Industry 4.0 Context. Sustainability, 2020, 12: 7066
2 Jadhav S D, Goossens L R, Kinds Y, et al. Laser-based powder bed fusion additive manufacturing of pure copper. Addit Manuf, 2021, 42: 101990
3 Jiang Q, Zhang P, Yu Z, et al. A review on additive manufacturing of pure copper. Coatings, 2021, 11: 740
4 Schubert T, Trindade B, Weißgärber T, et al. Interfacial design of Cu-based composites prepared by powder metallurgy for heat sink applications. Mater Sci Eng-A, 2008, 475: 39–44
5 Strondl A, Lyckfeldt O, Brodin H, et al. Characterization and control of powder properties for additive manufacturing. JOM, 2015, 67: 549–554
6 Li C, Li J, Hu Y, et al. Preparation and solidification process of mono-sized Cu–Ni–Sn microspheres by pulsated orifice ejection method. Mater Res Express, 2019, 6: 056517
7 Yang K, Fukumoto M, Yasui T, et al. Study of substrate preheating on flattening behavior of thermal-sprayed copper particles. J Therm Spray Tech, 2010, 19: 1195–1205
8 Watkinson J F. Atomization of metal and alloy powders. Powder Metallurgy, 1958, 1: 13–23
9 Soares Barreto E, Frey M, Wegner J, et al. Properties of gas-atomized Cu-Ti-based metallic glass powders for additive manufacturing. Mater Des, 2022, 215: 110519
10 Soong S Z, Lai W L, Kay Lup A N. Atomization of metal and alloy powders: processes, parameters, and properties. AIChE J, 2023, 69: e18217
11 Jeong S, Woo K, Kim D, et al. Controlling the thickness of the surface oxide layer on Cu nanoparticles for the fabrication of conductive structures by ink-jet printing. Adv Funct Mater, 2008, 18: 679–686
12 Zhou C, Qing F, Sun X, et al. Preparation of graphene-coated Cu particles with oxidation resistance by flash joule heating. Carbon, 2024, 224: 119060
13 Berry V. Impermeability of graphene and its applications. Carbon, 2013, 62: 1–10
14 Geim A K, Novoselov K S. The rise of graphene. Nat Mater, 2007, 6: 183–191
15 Bianco A, Cheng H M, Enoki T, et al. All in the graphene family – A recommended nomenclature for two-dimensional carbon materials. Carbon, 2013, 65: 1–6
16 Chen S, Brown L, Levendorf M, et al. Oxidation resistance of graphene-coated Cu and Cu/Ni alloy. ACS Nano, 2011, 5: 1321–1327
17 Zhao M, Zhang Z, Shi W, et al. Enhanced copper anticorrosion from Janus-doped bilayer graphene. Nat Commun, 2023, 14: 7447
18 Shu S C, Li Y H, Yan Z C, et al. Graphene-reinforced copper matrix composites as electrical contacts. ACS Applied Nano Materials, 2024, 7: 8685–8691
19 Ou H, Yan X, Wang C, et al. Chemical vapor deposition and applications of vertical graphene: progress and prospects (in Chinese). Chin Sci Bull, 2024, 69: 4748–4762 [区昊雄, 颜鑫承, 王超, 等. 站立式石墨烯的化学气相沉积及其应用: 现状与展望. 科学通报, 2024, 69: 4748–4762]
20 Qi Y, Sun L, Liu Z. Super graphene-skinned materials: an innovative strategy toward graphene applications. ACS Nano, 2024, 18: 4617–4623
21 Kim W J, Lee T J, Han S H. Multi-layer graphene/copper composites: preparation using high-ratio differential speed rolling, microstructure and mechanical properties. Carbon, 2014, 69: 55–65
22 Li J L, Xiong Y C, Wang X D, et al. Microstructure and tensile properties of bulk nanostructured aluminum/graphene composites prepared via cryomilling. Mater Sci Eng-A, 2015, 626: 400–405
23 Hwang J, Yoon T, Jin S H, et al. Enhanced mechanical properties of graphene/copper nanocomposites using a molecular-level mixing process. Adv Mater, 2013, 25: 6724–6729
24 Zeng M, Wang L, Liu J, et al. Self-assembly of graphene single crystals with uniform size and orientation: the first 2D super-ordered structure. J

Am Chem Soc, 2016, 138: 7812–7815
25 Zhang X, Xu Y, Wang M, et al. A powder-metallurgy-based strategy toward three-dimensional graphene-like network for reinforcing copper matrix composites. Nat Commun, 2020, 11: 2775
26 Lin Z, Shu S, Li A, et al. Preparation and mechanical property of graphene-reinforced copper matrix composites (in Chinese). J Inorg Mater, 2019, 34, 469–477 [林正得, 舒圣程, 李傲, 等. 石墨烯增强铜基复合材料的研究进展. 无机材料学报, 2019, 34: 469–477]
27 Hao C X, Wang X D, He Y, et al. PECVD synthesis of graphene toward wide applications: progress and prospects (in Chinese). Chin Sci Bull, 2024, 69: 1893–1905 [郝朝旭, 王雪东, 何燕, 等. 基于PECVD技术的石墨烯可控制备与应用: 现状与展望. 科学通报, 2024, 69: 1893–1905]
28 Wang S, Han S, Xin G, et al. High-quality graphene directly grown on Cu nanoparticles for Cu-graphene nanocomposites. Mater Des, 2018, 139: 181–187
29 Li T, Wang Y, Yang M, et al. High strength and conductivity copper/graphene composites prepared by severe plastic deformation of graphene coated copper powder. Mater Sci Eng-A, 2021, 826: 141983
30 Bao Q, Yang Y, Wen X, et al. The preparation of spherical metal powders using the high-temperature remelting spheroidization technology. Mater Des, 2021, 199: 109382
31 Schindelin J, Arganda-Carreras I, Frise E, et al. Fiji: an open-source platform for biological-image analysis. Nat Methods, 2012, 9: 676–682
32 Peng J, Chen B, Wang Z, et al. Surface coordination layer passivates oxidation of copper. Nature, 2020, 586: 390–394
33 Zhang M, Ye Q, Yu R, et al. *In-situ* conversion of amorphous carbon to graphene enhances the oxidation resistance of dendritic copper powder. Diamond Relat Mater, 2021, 120: 108695
34 Shtein M, Pri-Bar I, Varenik M, et al. Characterization of graphene-nanoplatelets structure via thermogravimetry. Anal Chem, 2015, 87: 4076–4080

Summary for “高温重熔化学气相沉积制备球形蒙烯铜粉”

Synthesis of spherical graphene-skinned copper powders by high-temperature remelting chemical vapor deposition

Wenxin Wu[1,2], Qingkang Feng[2], Xuhong Wu[3], Yifeng Zhao[4], Sijie Zhang[4], Zhiyuan Shi[4*], Xinli Guo[1*] & Qingkai Yu[2,4,5*]

[1] *Jiangsu Key Laboratory of Advanced Metallic Materials, School of Materials Science and Engineering, Southeast University, Nanjing 211189, China*
[2] *Shanghai CHechnology Co., Ltd., Shanghai 200444, China*
[3] *Shaanxi Sirui Advanced Materials Co., Ltd., Xi'an 710077, China*
[4] *State Key Laboratory of Materials for Integrated Circuits, Shanghai Institute of Microsystem and Information Technology, Shanghai 200050, China*
[5] *College of Materials Science and Opto-Electronic Technology, University of Chinese Academy of Sciences, Beijing 100049, China*
* Corresponding authors, E-mail: shizhy@mail.sim.ac.cn; guo.xinli@seu.edu.cn; qyu@mail.sim.ac.cn

The escalating demand for spherical copper powders in next-generation applications spanning additive manufacturing, flexible electronics (e.g., screen-printed stretchable circuits), and electrical contact systems (e.g., vacuum circuit breakers) necessitates the integration of high sphericity, superior flowability, and robust oxidation resistance. Yet, conventional manufacturing paradigms remain constrained, particularly due to the unavoidable coalescence of partially molten droplets. The coalescence results in irregular morphologies, excessive satellite particles, and broad-size distributions. Additionally, the sequential process of spheroidization followed by coating requires multi-step workflows involving sequential melting, solidification, surface activation, and coating, thereby introducing interfacial contamination risks and energy-intensive thermal cycling. Integrating functional coating layers during the spheroidization process offers a promising solution to minimize particle agglomeration and functionalize copper powder simultaneously. A graphene “skin” with poor wettability at copper interfaces not only prevents particle adhesion but also endows exceptional properties such as high electrical conductivity and oxidation resistance through its high electron mobility and barrier effect against water/oxygen permeation. In this study, an innovative high-temperature remelting chemical vapor deposition method was introduced. In a vertical reactor with an applied mild high-temperature field, copper feedstock descends through a vertical thermal gradient furnace while methane ascends under controlled flow. This configuration synergistically couples surface tension-driven spheroidization (where the particles are melted by heat exchange and molten copper droplets achieve near-ideal spherical geometry) with few-layered graphene growth (where methane cracking and carbon nucleation on the molten copper surface). The molten copper improves the diffusion and migration of carbon atoms, ensuring the supply of carbon atoms, and the liquid-phase surface also facilitates the rotation, alignment, and movement of graphene grains. In addition, the upward reaction atmosphere slows down the falling speed of copper powder and prolongs the gas-liquid interaction time. Experimental results demonstrate the successful production of highly spherical copper powder with sphericity reaching 0.89±0.11 at 1400°C. The graphene layers (fewer than 10 layers) are well aligned, and the carbon atoms in each layer are clearly distinguished through the transmission electron microscope, which suggests the good crystallinity of graphene. Towards the requirement of additive manufacturing or fusion-immersion sintering processes, two types of graphene-skinned copper powders with median particle size distributions in the range of 25–40 μm and 60–80 μm can be obtained after high-temperature growth. Comparative tests reveal that graphene-skinned copper powder exhibits significantly enhanced oxidation resistance compared to bare copper powder after NaOH corrosion or air oxidation treatments. The developed high-temperature remelting chemical vapor deposition technology enables continuous production of graphene-skinned copper powder with both high sphericity and elevated oxidation threshold temperature. This technique addresses critical limitations in traditional manufacturing approaches by integrating spheroidization and functionalization into a single-step process. The proposed strategy establishes a robust foundation for the mass production of high-performance spherical copper powder, potentially revolutionizing material supply for advanced applications.

chemical vapor deposition, graphene, spherical copper powder, oxidation resistance

doi: 10.1360/TB-2024-1404